

# Monitoring multiple damage mechanisms in crack-patched structures using optical infrared thermography

Ulrike Martens<sup>1</sup> and Kai-Uwe Schröder<sup>1</sup>

<sup>1</sup>RWTH Aachen University

July 1, 2020

## Abstract

The use of passive infrared thermography comprises great opportunities to improve understanding the fatigue damage process of crack-patched structures. Quasi-static and cyclic coupon tests are performed using metallic specimens with single-sided bonded patches and monitored with passive infrared thermography. Different test setups help to differentiate between metallic crack growth and adhesive damage on thermal images. Results show that metallic crack growth can be monitored from the patched side, also in combination with local delamination at the patch/metal interface. Thus, it is possible to analyse the overall degradation progress of the crack patched component under loading conditions and thereby to identify the driving damage mechanism of the particular repair configuration. Being able to understand the overall damage behaviour of crack patched components is essential to improve the ability of predicting its long-term behaviour.

## 1. Introduction

Metallic components exposed to cyclically varying loading tend to fatigue cracking. Adhesively bonded patches made of fibre reinforced plastics (FRP) are one repair solution that can significantly enhance the fatigue life of cracked metallic components. The repair basically consists of three major components, which are the cracked metallic structure, the FRP repair patch and the adhesive layer joining patch and the cracked component. The patch bridges the crack and loads that are applied to the metallic structure are transferred into the patch via the adhesive zone. The patch thereby reduces stresses at the crack tip which reduces crack growth. Additionally, due to the stiffening further crack opening is reduced, which again retards the crack growth. Even though crack growth can be theoretically be completely inhibited by a properly designed patch, see e.g. [1, 2, 3], cyclic mechanical loading and environmental influences cause material degradation resulting in further crack propagation during service [2, 4, 5]. But, even when the full patch functionality cannot be guaranteed, crack growth rates can still be reduced. However, for a repair with impaired functionality, the crack growth behaviour differs from theoretical performance predictions. To improve the prediction quality, it is essential to understand the damage processes under loading conditions.

For a patch repair, different damage mechanisms can occur. The two major damage mechanisms are metallic crack growth and local failure of the adhesive zone resulting in patch disbond and thereby reduced repair functionality. Depending on the repair configuration (stiffness ratio, application process, crack length, etc.) the driving damage mechanism can vary. The identification of the driving mechanism and possible mutual influences of the different damage mechanisms can be a significant factor to improve the patch design process, especially the quality of the performance prediction. As damage propagation is mainly a subsurface process, the use of non-destructive inspection (NDI) methods offers the ability to get an insight into the damage procedures of a crack patched structure under cyclic loading conditions. Optical infrared thermography (IrT) is one NDI technique commonly used in the detection of subsurface defects [6], also showing great applicability in the analysis of the damage behaviour of crack patched structures [7, 8]. The aim of this paper is to examine how IrT can help monitoring the cyclic heterogeneous damage propagation of crack

patched structures. The method used is passive IrT supported by optical lock-in thermography (LT), when necessary.

## State of the art in monitoring crack patching

For the “analysis, design and assessment of composite repairs” Jones et al. recommend among others the method of IrT as one NDI technique that is capable to picture damages. [7] Various studies on the potential capacity of IrT in the damage analysis of crack patched structures can be found in literature. The applicability of IrT methods for the assessment of bonded repair patches was shown for instance in [9], [10], and [11]. Avdelidis et al. analysed the capability of active thermography methods in detecting cracks and patch delamination [9] and Paipetis et al. showed the capability of LT to detect artificially introduced defects in the adhesive and between the patch layers [10]. Similar studies focussing on the repair assessment were carried out by Grammatikos et al. in [14] and Pavlopoulou et al. in [12]. Grammatikos et al. examined LT to assess the off-line and online characteristics for maintenance activities, while Pavlopoulou et al. compared LT to other NDI techniques as a possible structural health monitoring technique assessing the repair integrity under loading conditions. The ability using IrT methods for the analysis of the damage process was shown for instance by Avdelidis et al. [9, 13]. Grammatikos et al. further showed in [14] and [15] that LT can be used as a qualitative and quantitative approach to analyse the patch disbond process. Aiming on improving the predictability of the repair performance under service conditions, also the overall degradation process is of great interest. A preceding study, performed at the institute for structural mechanics and lightweight design (SLA), RWTH Aachen University, showed the great potential of using IrT for the analysis of subsurface damage propagation behaviour under mechanical loading.[8] The methods of passive IrT and optical LT were examined with respect to their ability to monitor the adhesive damage propagation process under quasi-static and fatigue loading. Results show that both thermography methods are able to picture the subsurface disbond propagation under loading conditions. The qualitative information given by the thermal images can be used to prove or disprove assumptions concerning the made during the design process. The method of passive IrT turned out to be much easier to handle. Therefore, also in this study mainly the method of passive IrT is used. The idea is to visualize the heterogeneous subsurface damage procedures of crack patched components under mechanical loading. The goal is to find out whether the different failure mechanisms can be distinguished on the thermal images and how the use of IrT can contribute to improve the prediction quality by an improved understanding of the damage processes.

## 2. Theory

For the interpretation of the test results, a short introduction into the functionality of IrT is provided.

### 2.1. Infrared thermography

In the present examination, passive IrT and supplementarily also optical LT are applied to monitor the damage behaviour of mechanically loaded crack patched specimens. A sketch of the test setup of IrT can be found in Fig. 1. On the right hand side the loaded specimen is depicted which sends varying infrared radiation due to varying loading.

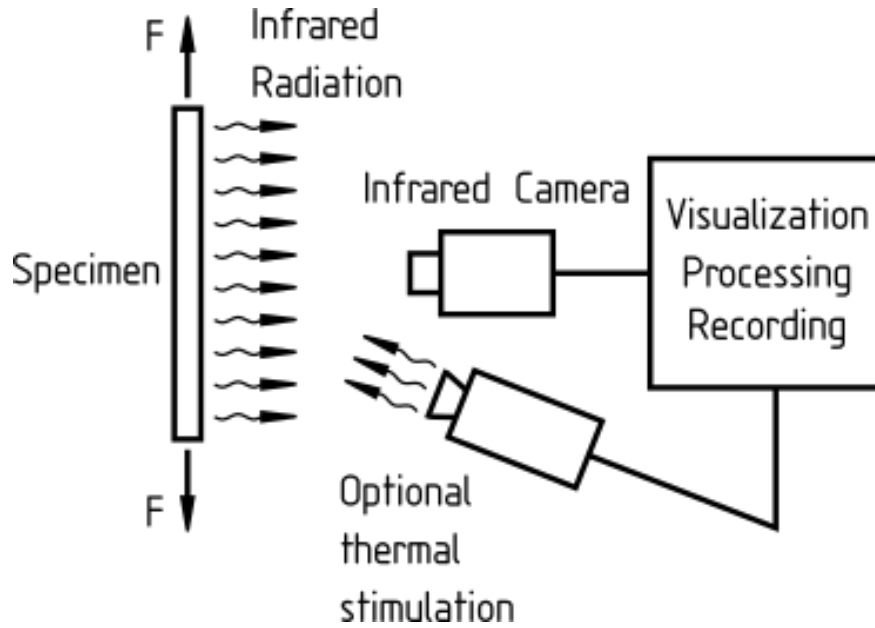


Fig. 1: IrT setup according to [6]

This infrared radiation is detected by the camera, which is connected to a processing unit that converts the radiation data into thermal images. An optional thermal stimulation unit is needed for active IrT methods. The method of passive IrT measures the temperature variations on the object's surface. Internal conversion processes for instance, that go along with (local) temperature changes can be detected measuring the attending changes in infrared radiation. Thereby, temperature hot spots resulting from crack formation and crack growth processes for instance can be detected. For more detailed information on IrT see [6].

Active IrT methods on the other hand use external excitation units for the thermal stimulation of the specimen. Optical LT for instance uses an external heat source, denoted as optional thermal stimulation in Fig. 1, introduces a heat flow into the specimen. The energy flow moves through the specimen and is partly reversed at material boundaries, such as voids or similar. The reversed energy flow is detected by the IrT camera system. Local differences in infrared radiation can thereby be visualized. This way, thermal images can be used to find subsurface irregularities.

## 2.2. Test Description

Two test series are performed, one under quasi-static and the other under fatigue loading. For each test, three different configurations are tested: specimens without patch, specimens with patch monitored from the metallic side and specimens with patch monitored from the patched side. The infrared camera used is of type ImageIR R 8380 S (InfraTec GmbH, Dresden) in combination with a tele zoom lens ( $f = 50$  mm). The test equipment used is a tensile and compression machine of type Instron 5567 (Instron, Darmstadt) for the quasi-static tests and a servo-hydraulic test machine of type Schenck POZ 160 with a static nominal load of  $\pm 160$  kN. For the quasi-static tests, a test velocity of 9 mm/min and a monitoring frame rate of  $f = 200$  Hz is used. The fatigue tests are performed with a stress ratio  $R = 0.1$ , mean load  $F_m = 4000$  N, load amplitude  $F_a = 3272$  N and a monitoring frame rate  $f = 100$  Hz. To reduce data, recording is done every 10000 load cycles for about 5 seconds.

All specimens are made of aluminium 5083 with a thickness of  $h = 3$  mm. The patch material used is a 0/90 epoxy-based carbon fibre reinforced plastic prepreg (SGL Technologies GmbH of type C W410-TW2/2-E323/42%/6k and a ply thickness of  $h = 0.6$  mm). Specimen geometries and dimensions are given in Fig. 2.

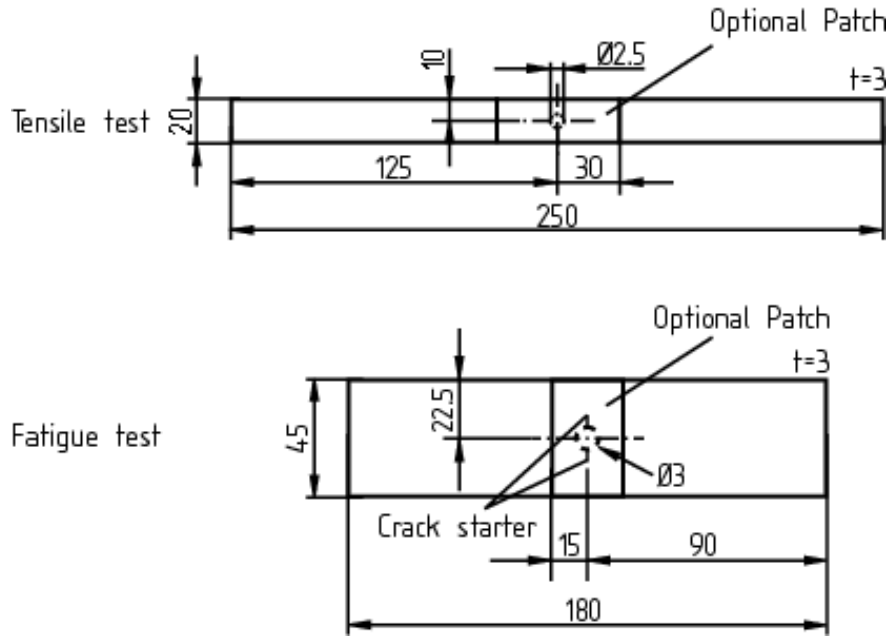


Fig. 2: Specimen geometries

For the fatigue specimens hand sawn cuts of 2 mm length each and placed perpendicular to the load direction act as a crack starter. Specimen preparation is kept simple since the focus lies on the monitoring methods and not on the patch performance. After cleaning the metal sheets with acetone, patches are directly bonded without using an extra adhesive layer. Specimens are heated in a temperature chamber ( $T = 100^{\circ}\text{C}$ ,  $t = 2 \text{ h}$ ) placed on a metallic sheet and covered by a plastic foil. A vacuum pump is applied throughout the heating process in order to create a proper bonding.

### 2.3. Preliminary estimations

At first, a metallic plate without mechanical loading is examined using optical LT. The aim of this preliminary test is to qualitatively find out whether or not it is possible to detect a crack in the metallic plate lying underneath a local defect in the adhesive layer. The specimen design can be seen in Fig. 3.

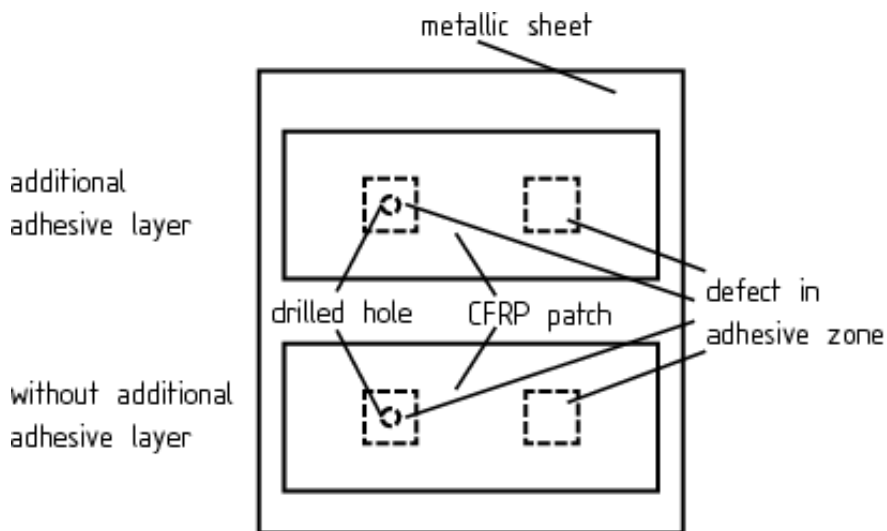


Fig. 3: Geometry preliminary test

One layer of a biaxial CFRP prepreg material is mounted on the metallic substrate to simulate the repair patch. The defect in the metallic plate is simulated by a drilled hole of 6 mm in diameter. Two different patch configurations are tested, one with an extra adhesive layer (DuploTEC 10400, Lohmann) and the other using the epoxy itself joining the components. A small square of newsprint is intentionally worked in the specimen between the patch and the metal to simulate local patch delamination.

For LT, the measurement depth is dependent on the lock-in frequency as well as the number of lock-in periods. The pure delamination defect on the right-hand side of the specimen is used to calibrate the camera for the defect depth. The second defect is a combination of local patch detachment and a defect in the metallic part simulated by a drilled hole underneath.

Fig. 4 shows the thermal images for the lock-in frequencies of  $f = 0.1$  Hz,  $f = 0.2$  Hz and  $f = 1$  Hz.

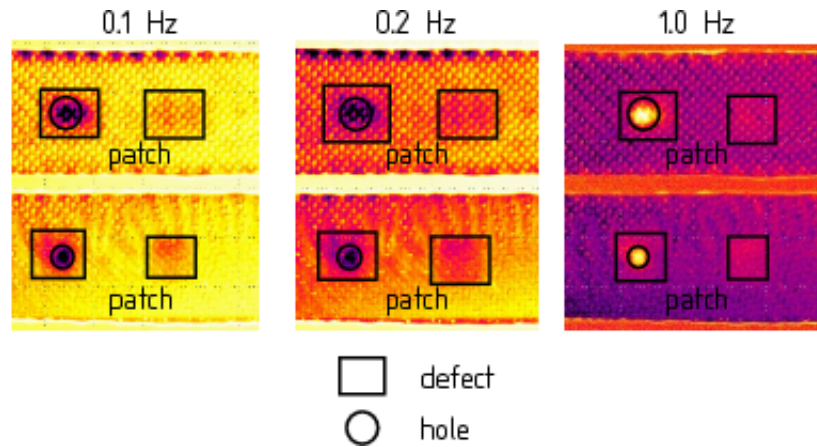


Fig. 4: Results preliminary test

For all frequencies tested, the square defect on the right-hand side of each picture can clearly be seen. On the left-hand sides, the square damage as well as the hole in the metal can be detected. This means, that the detection of both defect types is possible within a certain range of lock-in frequencies. It can further be seen that the outlines of the defects are more clearly visible for the lower configuration without an additional adhesive layer than for the upper one with an adhesive layer.

Nevertheless, for both configurations the defects are visible. As a conclusion one can say, that LT is generally capable to detect a damage in the metallic part of a patch repair that is lying underneath a local defect in the adhesive layer. Since a hole of 0.6 mm is not representable in dimension for a fatigue crack, the applicability of this method to detect small cracks thus needs to be further analysed. Statements concerning the influence of patch thickness cannot be made either so far.

### 3. Test Results

To find out if crack growth processes and patch delamination can be differentiated on thermal images, at first solely the crack growth process of metallic specimens without additional patches is monitored using passive IrT. In addition, patched specimens are monitored from the unpatched side to find out about possible differences caused by the patch. At last, specimens with patched are monitored from the patched side in order to monitor the overall damage progress.

#### 3.1. Quasi-static Loading

Specimens without and with FRP patches are loaded quasi-statically and damage behaviour is monitored using passive IrT. To measure temperature differences, three measurement fields are defined on the specimen

surface. The first above the hole for the minimum temperature and the second and third at the crack tips for the maximum temperature, see Figure 5.

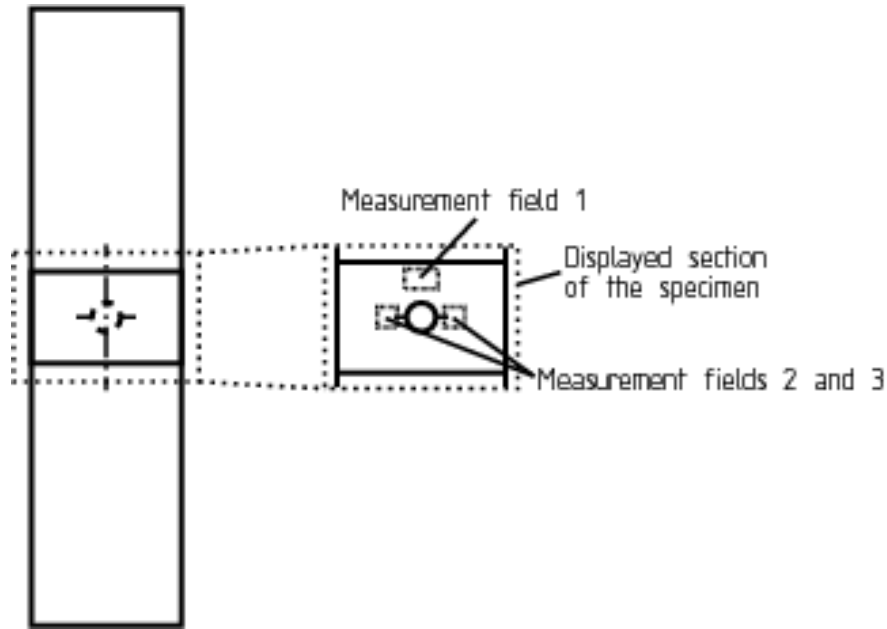


Figure 5: Displayed section of the specimen and measurement fields used to read out temperature values. Fields 2 and 3 move with the crack tips towards the specimen edges with increasing crack length. Maximum and minimum temperature values are read out by the software.

*Specimens without patch*

To get a first idea about the thermal behaviour of the metallic specimens under loading, quasi-static tests with metallic specimens are performed. Test evaluation shows that during the entire test, changes in the local temperature can be seen. After exceeding the linear-elastic region of the material, heat “flashes” can be seen on the thermal images as 45-lines to the loading direction, see Fig. 6.

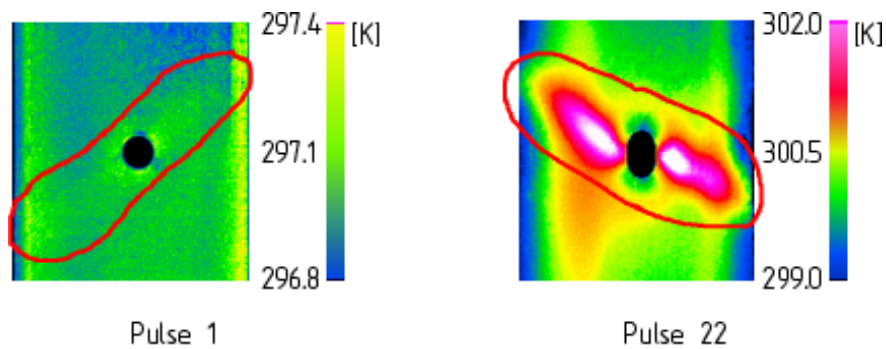


Fig. 6: First and one of the last detectable slip bands

The picture on the left-hand side shows the first detected pulse and the picture on the right-hand side one of the last ones. The load/displacement curve shown Fig. 7 helps to arrange the pulses within the test course.

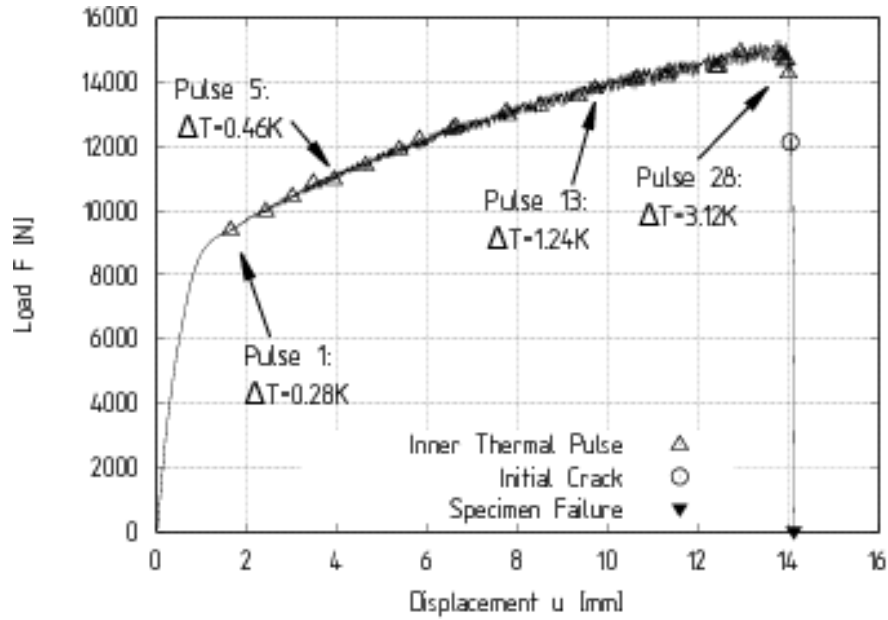
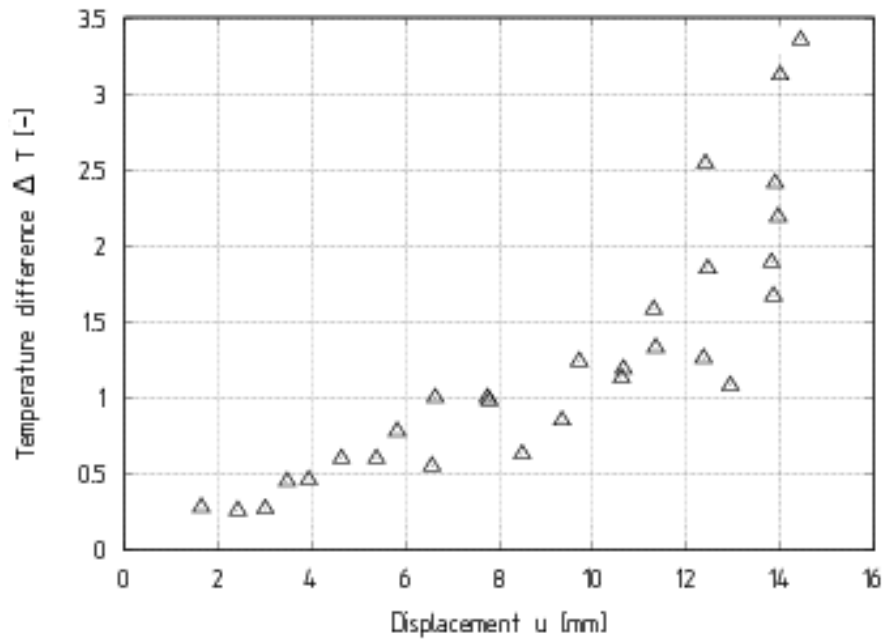


Fig. 7: Load/displacement curve for a specimen without patch

The course of the load/displacement curve is described by drops in the force signal that increase over time. The non-smooth load/displacement behaviour in the plastic region leads to the conclusion that this phenomenon can be related to the so-called “Portevin-Le Chatelier” (PLC) effect. The temperature “flashes” are slip bands running through the material. For more information on the PLC effect see for instance [16]. Number and size of the drops in the force signal correspond to the frequency and intensity of the detected slip bands running through the specimen. Monitoring the region around the hole, where crack onset is expected, the increase in number and intensity can be seen. Slip bands running through the hole pile up and local temperature differences increase over testing time, as shown in Fig. 8.



Φηγ. 8: Μαξίμνμ τεμπερατυρε δνφφερενζε  $\Delta T$  φορ εαση ηεατ πνλσε νδεντυφνεδ αροννδ τηε hole

The maximum temperature variation  $T$  is plotted against the overall displacement and each detectable pulse is marked with the symbol  $\circ$ . It has to be noted that with the used frame rate of  $f = 200$  Hz these bands can only be seen on 1-3 images. Therefore, possibly not all bands were detected. The first detectable pulse appears at a displacement less than 2 mm with a maximum  $T = 0.28$ K. With increasing displacement, the temperature difference increases up to  $T = 3.12$ K. The intensity of the first and last detectable slip band, as shown in Fig. 6, visualizes the increase in temperature with a maximum temperature difference of  $T = 0.28$ K for the first and  $T = 3.12$ K for the last one. This means that with increasing test progress also visibility improves.

Further, for the tensile test two characteristic thermal events can be monitored, see Fig. 9.

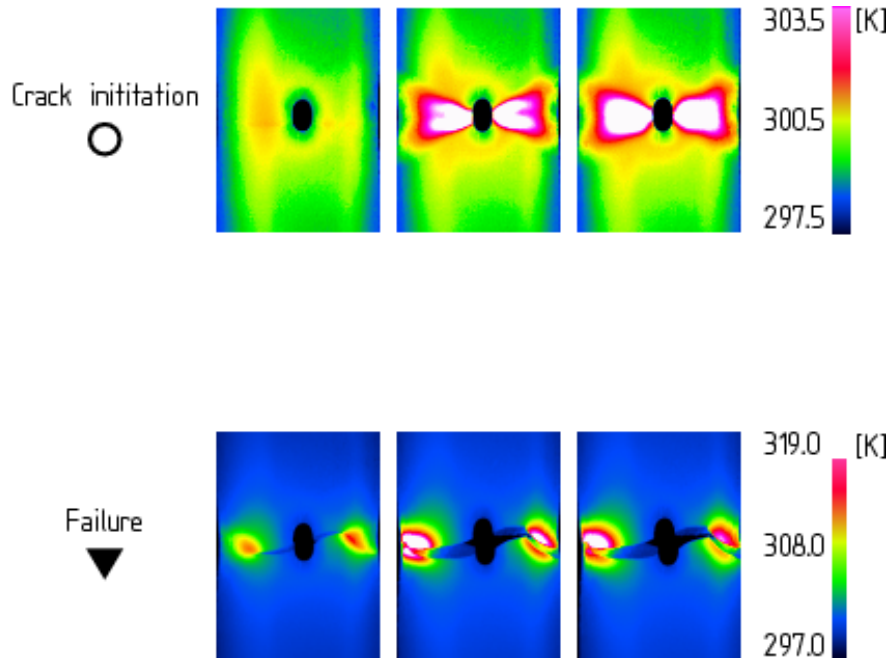


Fig. 9: Crack initiation and final failure

Right before crack initiation, marked with a  $\circ$ , a last high-intensity pulse runs through the hole (here, pulse 28). Final break is marked with the symbol  $\blacktriangledown$  in the load/displacement curve. At crack onset the heat increase at both sides of the hole is clearly detectable with a maximum temperature difference of  $T = 17.1$ K. Also, for final break, the crack tip running through the specimen is well-defined as a local temperature increase. The maximum temperature difference can be measured to be  $T = 36.47$ K.

#### *Specimens with patch*

Specimens with patch show a very similar load/displacement behaviour as the unpatched ones. Differences in elasticity between metal sheet and the rather stiff patch combined with the increasing strain lead to a patch detachment right after exceeding the linear-elastic region so that the stiffening effect of the patch cannot be monitored. In most test cases the patch detaches below the hole and sticks partly to the sheet above the hole. For the test evaluation this means that the patch still covers the hole but does not longer stiffen the specimen.

Analyses of the patched specimens monitored from the metallic side therefore do not give any considerable

additional information compared to the specimens without patch. A comparison of the load/displacement curves and the thermal images shows that the damage behaviour including the characteristic events of specimen failure are comparable. The patch detaches in a one- or two-stage process resulting in one or two additional characteristic event(s) in the load/displacement curve, as shown in Fig. 10, denoted with the symbols  $\square$  and  $\diamond$ .

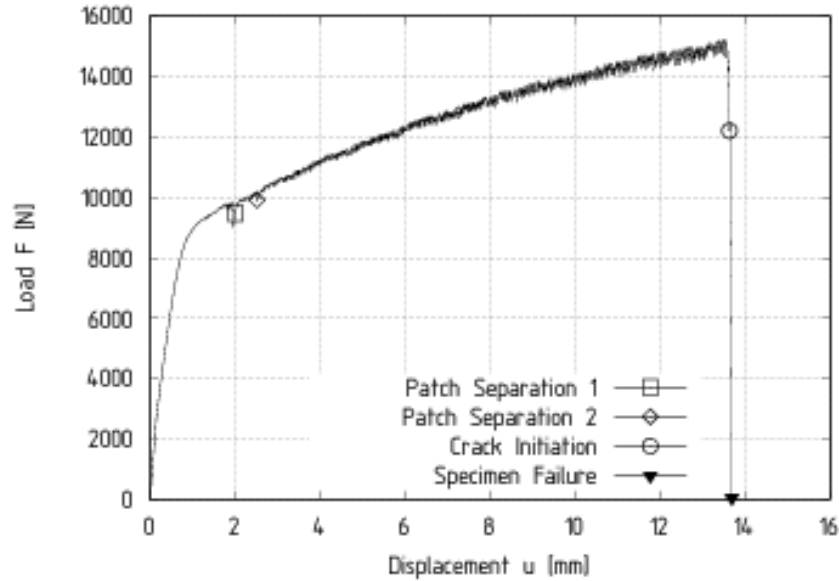


Fig. 10: Load/displacement curve for a specimen with patch

Knowing the load/displacement behaviour and at which points irregularities that go along with an increase in temperature helps to understand thermal images taken from the patched side. Correlating thermal images with the test curve helps to find thermal images taken at the characteristic events monitored from the patched side, as shown in Fig. 11.

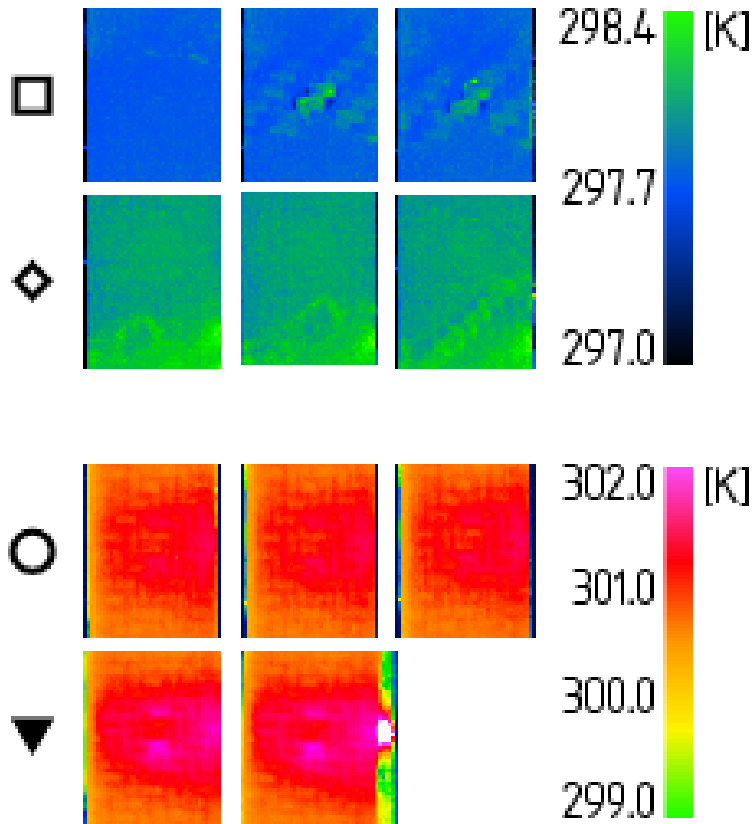


Fig. 11: Patch detachment 1 and 2 , crack initiation and final failure

Again, the images show the region around the hole which is covered by the CFRP patch and whose woven structure can be identified. For each event three consecutive images are shown that are found to be taken close to the characteristic events.

The two points of patch detachment (  $\square$  and  $\diamond$  ) show a slight diagonal increase in temperature around the central hole. In the first row two diagonal lines can be seen and in the second one only one line. It seems that these temperature increase can be related to metallic slip bands. But it actually cannot clearly be said whether these lines of increased temperature result from diagonal slip bands or from the diagonal structure of the patch.

Considering crack initiation (  $\circ$  ) and final failure (  $\blacktriangledown$  ), an increase in temperature can be seen through the patch in the specimen centre. As the patch is already detached around the hole, outlines are blurred and only a non-specific field of increased temperature can be made out. The temperature difference here lies at around  $T = 45$  at the patch surface, compared to a  $T = 7.1\text{K}$  for the temperature increase measured at the metallic surface. The very last picture covers the moment of patch detachment. The actual temperature increase around the hole can be seen at the right-hand side where the metal sheet is not covered by the patch. While the temperature difference is more than  $T = 8\text{K}$  at the edge of the metallic part, on the patch surface only difference of around  $T = 2.59\text{K}$  is detectable.

### 3.2. Fatigue Loading

Compared to the quasi-static tests, under cyclic loading different conditions apply. Fatigue crack growth

differs from static failure. The main difference is that cracks grow at lower stresses and, more important here, lower strains. This means that also temperature evaluation is less than for static damage. Further, due to the continuous loading and unloading, temperature does not solely increase because of plastic deformation at the stress peaks, but also globally due to internal friction. Cyclic loading leads to molecular movements inside the material. Thereby, the entire specimen heats up over testing time. Therefore, temperature differences  $T$  are expected to be small. On the other hand, due to smaller deformations, sudden patch detachment is not expectable. A proper bonding leads to improved visibility of the subsurface phenomenae.

Thermal images of one exemplarily chosen unpatched specimen, shown in Fig. 12, depict the temperature development during crack propagation for four exemplarily chosen numbers of load cycles  $N$ .

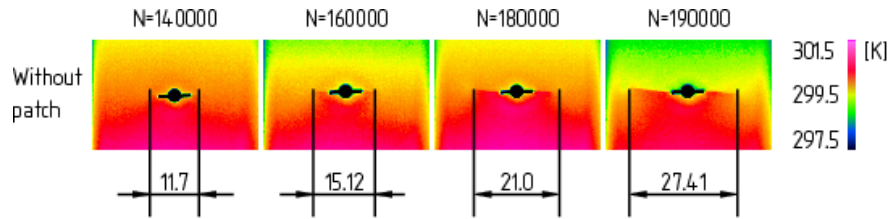


Fig. 12: Crack propagation process for an unpatched under fatigue loading

Monitoring the metallic crack growth with passive IrT shows that the longer the crack grows, the better it can be made out on the thermal image. For small crack lengths on the other hand, crack tip detection can be difficult. One reason might be, that the movement of the lower piston heats up the specimen during testing. Temperature thus increases from the bottom to the top and the crack acts as a heat barrier. The bigger the temperature differences become over time, the easier cracks can be made out. Moreover, a circular area around the crack tip can be identified which builds up during loading and vanishes while unloading the specimen. This area helps to identify the crack tip and thereby to measure the crack length.

As for the quasi-static test, differences between the images from the unpatched specimen and the ones with patch monitored from the metallic side are neglectable. Fig. 13 shows the temperature evaluation for two patched specimens, one monitored from the metallic side and the other from the patched one.

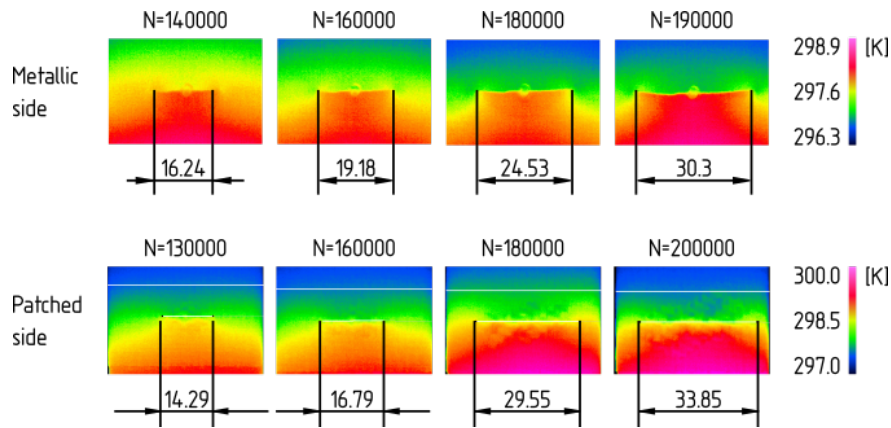


Fig. 13: Comparison crack propagation process for two patched specimens under fatigue loading monitored from the metallic and the patched side

Understanding the interaction between local patch detachment and crack growth in the structure is one essential goal in the patch design process. To find out, how these two effects influence one another can lead to improved design methods. Therefore, additional investigations using optical LT are made for the specimen

that is monitored from the patched side. A comparison of the thermal images gained from passive IrT and phase images resulting from LT measurements are displayed in Fig. 14.

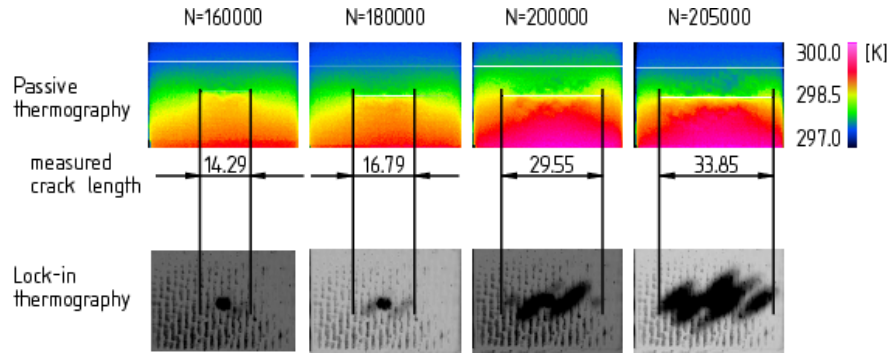


Fig. 14: Comparison crack propagation process using passive IrT and LT

Local patch detachment can be made out as dark spots on the phase images, comparable in size and contour lines with the results gained from passive IrT. The crack on the other hand cannot be identified on the phase images.

#### 4. Discussion

Under quasi-static loading, the knowledge of local temperature changes helps understanding the thermal examination through the bonded patch. Monitoring a patched specimen, sudden local temperature increases at an angle of around  $45^\circ$  to the loading direction, combined with noise effects in the load/displacement curve can thus be allocated to the PLC effect. An increase of the effect over time is measurable. Compared to the specimens without patch the detectable temperature difference from the patched side is reduced, because temperature differences are rather small, and the resulting infrared radiation is weakened by the CFRP patch. Additionally, temperature flashes run suddenly through the specimen so that a clear identification of damage initiation through the patch is difficult. Further, due to the local patch detachment the air between the patch and the specimen additionally influences the radiation intensity. For patches of one layer of the chosen CFRP material, subsurface effects which are related to heat generation can generally be identified on thermal images. But, temperature difference  $T$  has to be high enough. The origin of heat generation cannot clearly be identified without further information. Interpretation of thermal images needs for additional knowledge resulting from the stress/strain behaviour e.g.

For specimens loaded in fatigue, results are different. Crack length measurement is possible from the metallic side and becomes even better, the longer the crack growth. As the specimens are loaded by the lower piston, they heat up from the bottom to the top. The temperature difference between the upper and the lower part of the specimen increases with increasing number of load cycles. As the heat circles the crack the crack itself acts as a temperature barrier and becomes visible through the temperature difference of the metallic part above and the one below the crack. From the patched side it is not as clear, but a good qualitative estimation is possible as well. Further, under cyclic loading, crack growth additionally goes along with local patch detachment, leading to a further reduction of crack detectability. A comparison of the results monitored from the metallic and from the patched side shows that crack length detection is possible from both sides. As seen for the unpatched specimen, a discontinuous temperature distribution appears around the crack tips with a maximum temperature increase  $T$  at the peak stress of each loading/unloading cycle. Using this top dead centre for test evaluation, crack tips can be identified also from the patched side. Imaging frequency should therefore be higher than test frequency so that it can be made sure that pictures at or close to the top dead centre are available. Unlike for the quasi-static loading, here, the measured temperature of the metallic and the patched side do not differ strongly, as long as there is a proper bonding between patch and specimen. Increasing local damages in the adhesive layer have an impact on the thermal properties

resulting in decreasing visibility of the crack. Local patch delamination can be identified on the thermal image as areas where the woven structure of the patch is noticeable. But still, crack propagation process can be monitored. Comparing crack length and detachment dimensions it seems that right in front of the crack the patch has already delaminated from the metal. Meaning that for the given specimen configuration and the given conditions presumably delamination around the crack tip appears before the crack grows. To further corroborate this hypothesis additional tests using complementary monitoring techniques have to be made.

## 5. Conclusions

When analyzing the damage processes of crack patched structures under quasi-static and cyclic loading, passive IrT is a good opportunity to help understanding the complex failure behaviour. From the unpatched side, of course, the metallic crack growth can be monitored easily, while it is more difficult from the patched one. For quasi-static loading big strain differences lead to extensive patch delamination which strongly detracts the thermal analysis. Fatigue loading on the other hand goes usually along with only local patch detachment. And, as long as the patch is bonded to the specimen for the most part, and temperature changes can be made out on the patch surface, also the subsurface crack growth process can be monitored. Due to the overall increase in temperature, crack detectability improves over time. On the other hand, with increasing local delamination image interpretation becomes more difficult. Here, at maximum load, crack length can even be measured for locally detached patches. In total, the method of IrT provides the opportunity to gain a better understanding of the fatigue behaviour of crack patched structures.

Additional tests are needed to proof whether patches made of several layers still lead to utilizable thermal images and how an additional adhesive layer influences the results. Provided that the temperature increase must be strong enough to be detectable on the patch surface, passive IrT can help understanding the degradation process of a crack patched structure under long-term loading. The design assumption commonly used that a proper bonding is present, is usually not given under service conditions. Even for patch application under laboratory conditions long-term loading and environmental influences degrade the mechanical properties of the adhesive. Thus, designing the patch using ideal bonding conditions can lead to false assessments in the performance prediction. In forthcoming studies, the method of passive IrT can be used to describe the damage behaviour of crack patched components more realistically. The method of passive IrT comprises the possibility to identify the component (metallic sheet, adhesive zone, or patch) where the first damage onset occurs and how the different damage mechanisms influence one another. Thereby it provides great potential for improving the patch design process and to make failure prediction more reliable.

## References

- [1] Baker AA, Jones LR. *Bonded Repair of Aircraft Structures* : Springer Science & Business Media; 1988.
- [2] Baker AA, Francis LR, Jones R. *Advances in the bonded composite repair of metallic aircraft structure* : Elsevier; 2003. doi:10.1016/B978-008042699-0/50000-0.
- [3] Duong CN, Wang CH. *Composite repair: theory and design* : Elsevier; 2010. doi:10.1016/B978-008045146-6/50001-1.
- [4] Baker AA, Rajic N, Davis C. Towards a practical structural health monitoring technology for patched cracks in aircraft structure. *Composites Part A: Applied Science and Manufacturing* 2009; 40 (9): 1340–1352. doi:<https://doi.org/10.1016/j.compositesa.2008.09.015?nosfx=y>
- [5] Schubbe JJ, Bolstad SH, Reyes S. Fatigue crack growth behavior of aerospace and ship-grade aluminum repaired with composite patches in a corrosive environment. *Composite Structures*: 2016; 144: 44–56.
- [6] Maldague X. *Theory and practice of infrared technology for nondestructive testing* . Wiley; 2001.
- [7] Jones R, Baker AA, Matthews N, Champagne V. *Aircraft sustainment and repair* . Butterworth-Heinemann; 2017. doi:10.1016/B978-0-08-100540-8.09992-1.

- [8] Martens U, Schröder K-U. Evaluation of infrared thermography methods for analysing the damage behaviour of adhesively bonded repair solutions. *Composite Structures*: 2020; 240. doi:<https://doi.org/10.1016/j.compstruct.2020.111991>
- [9] Avdelidis NP, Moropoulou A, Riga ZM. The technology of composite patches and their structural reliability inspection using infrared imaging. *Progress in aerospace Sciences* ; 2003; 39 (4): 317–328.
- [10] Paipetis AS, Grammatikos SA, Kordatos EZ, Barkoula N-M, Matikas TE. In service damage assessment of bonded composite repairs with full field thermographic techniques. In: *Nondestructive Characterization for Composite Materials, Aerospace Engineering, Civil Infrastructure, and Homeland Security* . San Diego: International Society for Optics and Photonics; 2011:79831U. doi:10.1117/12.880376.
- [11] Moropoulou A, Avdelidis NP. Active thermography in the assessment of repaired aircraft panels. *Insight* 2002; 44: 145-149.
- [12] Pavlopoulou S, Grammatikos SA, Kordatos EZ, Worden K, Paipetis AS, Matikas TE, Soutis C. Continuous debonding monitoring of a patch repaired helicopter stabilizer: Damage assessment and analysis. *Composite Structures* ; 2015; 127: 231–244.
- [13] Avdelidis NP, Ibarra-Castanedo C, Maldague X, Almond DP, Moropoulou A. Thermal NDT & E of composite aircraft repairs. In: *16th WCNDT 2004*. Montreal: World Conference on NDT; 2004:TS4.27.3: 1-9.
- [14] Grammatikos SA, Kordatos EZ, Aggelis DG, Matikas TE, Paipetis AS. Critical and subcritical damage monitoring of bonded composite repairs using innovative non-destructive techniques. In: *Smart Sensor Phenomena, Technology, Networks, and Systems Integration* . San Francisco: International Society for Optics and Photonics; 2012: 834611.
- [15] Grammatikos SA, Kordatos EZ, Matikas TE, Paipetis AS. On the fatigue response of a bonded repaired aerospace composite using thermography. *Composite Structures*: 2018; 188: 461–469. doi: <https://doi.org/10.1016/j.compstruct.2018.01.035>.
- [16] Kubin LP, Ananthakrishna G, Fressengeas C. Comment on “Portevin–Le Chatelier effect”. *Physical Review E*; 2002; 65. doi: <https://doi.org/10.1103/PhysRevE.65.053501>.

### Source of Funding

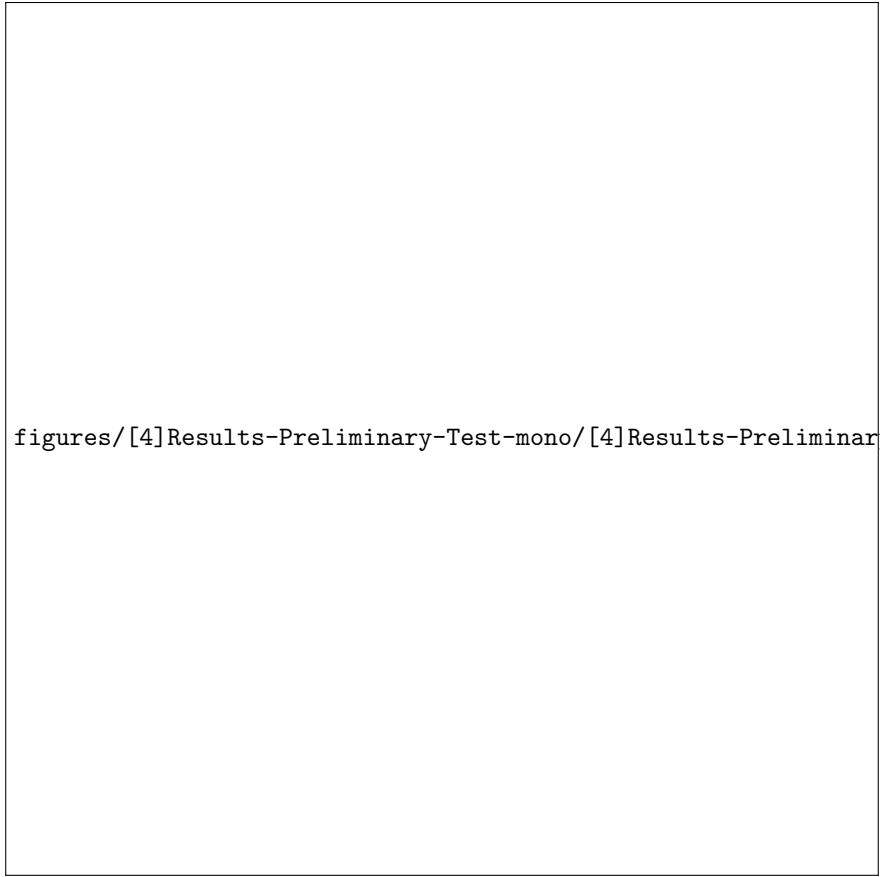
None

### Conflict of interest

None

figures/[3]Geometry-Preliminary-Test/[3]Geometry-Preliminary-Test-eps-converted-to.pdf

figures/[4]Results-Preliminary-Test/[4]Results-Preliminary-Test-eps-converted-to.pdf



figures/[4]Results-Preliminary-Test-mono/[4]Results-Preliminary-Test-mono-eps-converted-t

figures/[6]Slip-Bands/[6]Slip-Bands-eps-converted-to.pdf

figures/[6]Slip-Bands-mono/[6]Slip-Bands-mono-eps-converted-to.pdf

figures/[9]No-Patch-CI-FF/[9]No-Patch-CI-FF-eps-converted-to.pdf

figures/[9]No-Patch-CI-FF-mono/[9]No-Patch-CI-FF-mono-eps-converted-to.pdf

figures/[10]LD-Curve-Patch/[10]LD-Curve-Patch-eps-converted-to.pdf

figures/[11]Patch-CI-FF/[11]Patch-CI-FF-eps-converted-to.pdf

figures/[11]Patch-CI-FF-mono/[11]Patch-CI-FF-mono-eps-converted-to.pdf

figures/[12]Crack-Propagation-No-Patch/[12]Crack-Propagation-No-Patch-eps-converted-to.pdf

figures/[12]Crack-Propagation-No-Patch-mono/[12]Crack-Propagation-No-Patch-mono-eps-conve

figures/[13]Comparison-Patch-Metal/[13]Comparison-Patch-Metal-eps-converted-to.pdf

figures/[13]Comparison-Patch-Metal-mono/[13]Comparison-Patch-Metal-mono-eps-converted-to.

figures/[14]Comparison-PT-LT/[14]Comparison-PT-LT-eps-converted-to.pdf

figures/[14]Comparison-PT-LT-mono/[14]Comparison-PT-LT-mono-eps-converted-to.pdf